On the peak in the far-infrared conductivity of strongly anisotropic cuprates

A. Pimenov,[1] A. V. Pronin,[1, *] A. Loidl,[1] A. Tsukada,[2] and M. Naito[2]

[1]*Experimentalphysik V, Elektronische Korrelationen und Magnetismus,*
Institut für Physik, Universität Augsburg, 86135 Augsburg, Germany
[2]*NTT Basic Research Laboratories, 3-1, Morinosato-Wakamiya, Atsugi-shi, Kanagawa 243-0198, Japan*
(Dated: February 1, 2008)

We investigate the far-infrared and submillimeter-wave conductivity of electron-doped $La_{2-x}Ce_xCuO_4$ tilted $1°$ off from the ab-plane. The effective conductivity measured for this tilt angle reveals an intensive peak at finite frequency ($\nu \sim 50\,cm^{-1}$) due to a mixing of the in-plane and out-of-plane responses. The peak disappears for the pure in-plane response and transforms to the Drude-like contribution. Comparative analysis of the mixed and the in-plane contributions allows to extract the c-axis conductivity which shows a Josephson plasma resonance at $\nu \simeq 11.7\,cm^{-1}$ in the superconducting state.

Far-infrared conductivity in the normally-conducting state of the high-T_c cuprates can be well characterized by the Drude-like response [1]. This response leads to the levelling-off of the real part of the conductivity $\sigma^* = \sigma_1 + i\sigma_2$ in the submillimeter frequency range [2, 3]. In some cases deviations from this behavior can be observed in the conductivity spectra as broad maxima at far-infrared frequencies. One possible reason for such additional excitation can be a charge localization induced by doping [4]. More generally, disorder, such as inhomogeneous oxygen distribution [5, 6, 7], has been shown to lead to a an additional maximum in conductivity [8]. Further possible effects leading to a conductivity peak include charge density waves [9] or reduced dimensionality in the static stripe phase [10].

In this paper we present another possible mechanism for finite-frequency peak in the infrared conductivity of electron-doped cuprate $La_{2-x}Ce_xCuO_4$ (LCCO). The same arguments will hold for strongly anisotropic, mostly two-dimensional metals in which the out-of-plane response is nearly insulating. In the present case the peak arises due to a small admixture of the c-axis response to the in-plane conductivity. Rotating the polarization of the infrared radiation, the pure in-plane response can also be measured. The in-plane conductivity shows no infrared peak and follows the predictions of the Drude model. The comparative analysis of the spectra for different experimental geometries allowed to extract conductivity and dielectric constant along the c-axis.

$La_{2-x}Ce_xCuO_4$ film with $x = 0.075$ was deposited by molecular-beam epitaxy [11, 12] on transparent $SrLaAlO_4$ substrate $10 \times 10 \times 0.5$ mm^3 in size. The thickness of the film was 140 nm and the film revealed a sharp transition ($\Delta T_c < 1\,K$) at 25 K. Lower transition temperature compared to the optimally-doped compound ($T_c = 30\,K$) [12] and low Ce-concentration indicate the underdoped regime in the film. The $SrLaAlO_4$ has been cut close to the (001)K direction with the misfit

angle of $\alpha = 1° \pm 0.1°$. In this case the film grows nearly c-axis oriented with the same off-axis tilt-angle.

In order to obtain the complex conductivity in the frequency range from submillimeter-waves to far-infrared, two different experimental methods [13] have been applied to the same film. For frequencies below $40\,cm^{-1}$ the complex conductivity of the film has been obtained by the submillimeter transmission spectroscopy [14]. At higher frequencies the sample reflectance has been measured using standard far-infrared techniques and the conductivity was obtained via a Kramers-Kronig analysis of the spectra.

The transmission experiments for frequencies $5\,cm^{-1} < \nu < 40\,cm^{-1}$ were carried out in a Mach-Zehnder interferometer arrangement [14] which allows both, the measurements of the transmittance and the phase shift of a film on a substrate. The properties of the blank substrate were determined in a separate experiment. Utilizing the Fresnel optical formulas for the complex transmission coefficient of the substrate-film system, the absolute values of the complex conductivity $\sigma^* = \sigma_1 + i\sigma_2$ were determined directly from the measured spectra. In the frequency range $40 < \nu < 4000\,cm^{-1}$ reflectivity measurements were performed using a Bruker IFS-113v Fourier-transform spectrometer. In addition, the reflectance for frequencies $5 < \nu < 40\,cm^{-1}$ has been calculated from the complex conductivity data of the same sample, obtained by the submillimeter transmission. This substantially improves the quality of the subsequent Kramers-Kronig analysis of the reflectance and therefore the reliability of the data at the low-frequency part of the infrared spectrum.

Due to the tilt-structure of the film, two main experimental geometries are possible. Both cases are depicted in Fig. 1. In the first case (upper drawing) the currents, induced by the incident radiation, are within the CuO_2 plains only. Therefore, the pure in-plane response is obtained in this case. In the other experimental geometry (lower drawing in Fig. 1) a small admixture of the c-axis response is expected.

Figure 1 shows the far-infrared reflectance of the LCCO film for both possible experimental geometries.

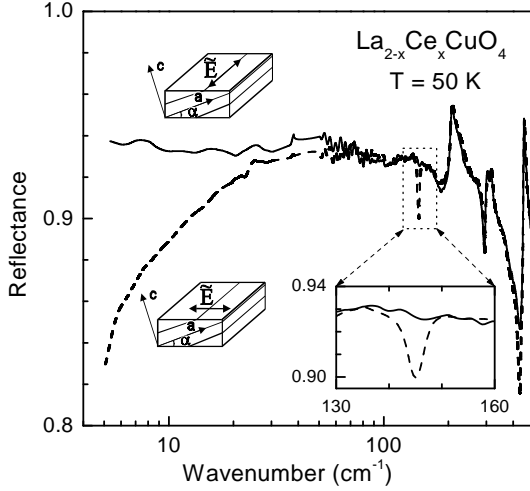*permanent address: General Physics Institute of the Russian Acad. of Sciences, 119991 Moscow, Russia

FIG. 1: Far-infrared reflectance of an underdoped LCCO film at different experimental geometries at $T = 50$ K. Solid lines - pure in-plane response, dashed lines - tilted geometry. The reflectance data above $40\,\mathrm{cm}^{-1}$ were measured directly and the spectra below this frequency were calculated from the complex conductivity data obtained by the transmittance technique. The inset shows the magnified spectra around a longitudinal c-axis phonon.

Sharp structures above $200\,\mathrm{cm}^{-1}$ are attributed to the phonons in the substrate. In that case no substantial difference is seen between the reflectance in both geometries. In addition to these effects, sharp minima in reflectance can be observed, which reveal a clear polarization dependence. One of such resonances is shown in the inset. We interpret these resonances as LO phonons in LCCO. The most important differences between the spectra of both geometries are seen below $50\,\mathrm{cm}^{-1}$: the spectra of the mixed geometry deviate significantly for decreasing frequencies.

The reflectivity of a thin metallic film on a dielectric substrate can be obtained from the Maxwell equations [15]:

$$r = \frac{r_{0f} + r_{fs}\exp(4\pi i n_f d/\lambda)}{1 + r_{0f}r_{fs}\exp(4\pi i n_f d/\lambda)} \quad , \qquad (1)$$

with $r_{0f} = (1-n_f)/(1+n_f)$ and $r_{fs} = (n_f-n_s)/(n_f+n_s)$ being the Fresnel reflection coefficients at the air-film (r_{0f}) and film-substrate (r_{fs}) interfaces. Here $n_f = (i\sigma^*/\varepsilon_0\omega^*)^{1/2}$ and n_s are the complex refractive indices of the film and substrate, respectively, λ is the radiation wavelength, d is the film thickness, $\omega = 2\pi\nu$ is the angular frequency, $\sigma^* = \sigma_1 + i\sigma_2$ is the complex conductivity of the film, and ε_0 is the permittivity of free space. Eq. (1) is written neglecting the multiple reflections from the opposite sides of the substrate. If the film thickness is smaller than the penetration depth ($|n_f|\,d \gg \lambda$) and if $|n_f| \gg |n_s|$, Eq. (1) can be simplified to :

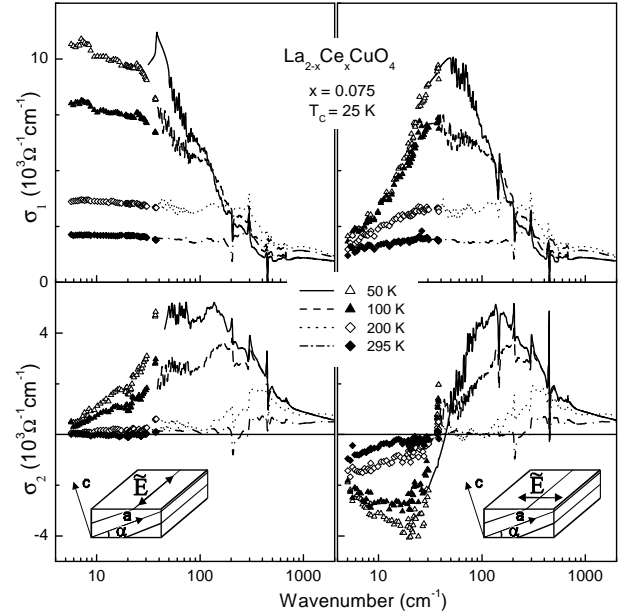$$r \approx \frac{1 - \sigma^* d Z_0 - n_s}{1 + \sigma^* d Z_0 + n_s}, \qquad (2)$$

FIG. 2: Far-infrared conductivity of LCCO film for two different experimental geometries as indicated in the insets. Upper panels - σ_1, lower panels - σ_2. Left panels: in-plane response, right panels: mixed ac-geometry. Lines represent the conductivity obtained from the infrared reflectance, symbols - the conductivity as measured directly by the submillimeter transmission technique.

where $Z_0 = \sqrt{\mu_0/\varepsilon_0} \simeq 377\,\Omega$ is the impedance of free space.

Figure 2 shows the far-infrared conductivity of LCCO. The results above $40\,\mathrm{cm}^{-1}$ were obtained applying the Kramers-Kronig analysis to the reflectivity data and solving Eq. (1). Below $40\,\mathrm{cm}^{-1}$ the complex conductivity was calculated directly from the transmittance and phase shift. The far-infrared conductivity of LCCO for the in-plane response (left panels) resembles well the predictions of the Drude model. At low frequencies, σ_1 is frequency independent and σ_2 increases approximately linearly with the frequency. For frequencies close to the value of the scattering rate, σ_1 starts to decrease and σ_2 shows a maximum, $\nu_{max} \simeq 1/2\pi\tau$. On the contrary, the $1°$ tilted geometry (right panels) reveals dramatic changes compared to the in-plane response. The real part of the conductivity shows an intensive peak in the far-infrared range. As expected by the causality principle (via the Kramers-Kronig relations) the imaginary part of the conductivity for the tilted geometry shows a step-like structure at the same frequency. Fig. 2 demonstrates that already $1°$ off-axis geometry significantly modifies the low-frequency conductivity spectra. However, we note that the most significant changes appear in the low-frequency range, $\nu < 100\,\mathrm{cm}^{-1}$. The high-frequency response of the tilted geometry approximately follows the spectra of the CuO_2 planes.

In order to understand the off-axis response we utilize a simple model which takes into account a tilted geometry
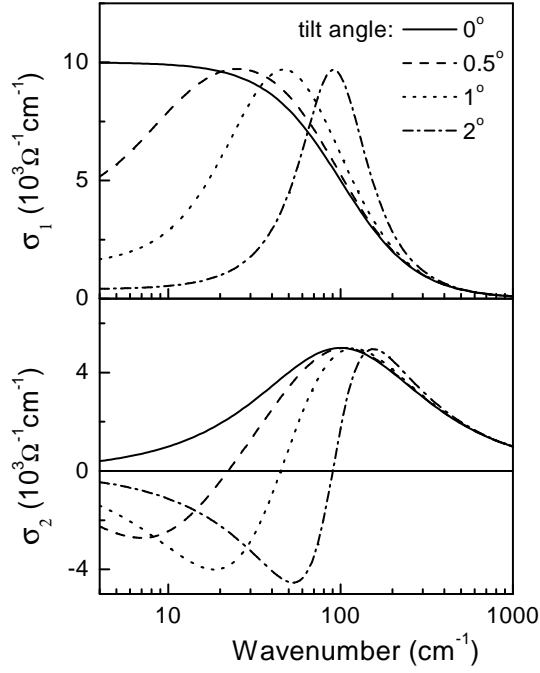
FIG. 3: Far-infrared conductivity of a tilt anisotropic sample as calculated from Eq. 3. The in-plane conductivity was assumed to obey the Drude-form with $\sigma_0 = 10^4\,\Omega^{-1}cm^{-1}$, $1/2\pi\tau = 100\,cm^{-1}$, and the c-axis response was taken as $\sigma_{1,c} = 0.5\,\Omega^{-1}cm^{-1}$ and $\varepsilon_{1,c} = 8$.

of the experiment [3, 16]. The model has been developed in the assumption that the penetration depth is mich smaller than the film thickness. This approximation for the effective conductivity is fulfilled in the present case and contains the essential physics of the problem. The conductivity of a thin film tilt by an angle α reads:

$$\sigma_{eff} = \frac{-i\varepsilon_0\omega(\sigma_a\cos^2\alpha + \sigma_c\sin^2\alpha) + \sigma_a\sigma_c}{-i\varepsilon_0\omega + \sigma_a\sin^2\alpha + \sigma_c\cos^2\alpha} \quad . \quad (3)$$

Here σ_a and σ_c are the complex conductivities in the CuO_2-planes and along the c-axis, respectively. Within the approximation $\alpha \approx \sin\alpha \ll 1$ and $|\sigma_a| \gg |\sigma_c|$, Eq. (3) can be rewritten as:

$$\frac{1}{\sigma_{eff}} = \frac{\alpha^2}{\sigma_c - i\varepsilon_0\omega} + \frac{1}{\sigma_a} \quad . \quad (4)$$

To understand the spectra in Fig. 2 qualitatively, the c-axis response of LCCO can be taken as purely insulating with a dielectric constant $\varepsilon_c \simeq 10$. In that case $\sigma_c \simeq -i\varepsilon_c\varepsilon_0\omega$ and the first term in Eq. 4 dominates the response for the tilted geometry below $\omega/2\pi \simeq \sigma_a\alpha^2/(\varepsilon_c\varepsilon_0) \simeq 20\,cm^{-1}$, which roughly corresponds to the conductivity maximum in the right upper panel of Fig. 2.

Figure 3 shows the conductivity of a tilted sample as calculated on the basis of Eq. 3 and for different tilt angles α. The parameters of the model have been taken to

correspond to the $T = 50\,K$ data in Fig. 2. The in-plane conductivity was assumed to obey the Drude-form $\sigma^* = \sigma_0/(1 - i\omega\tau)$ with $\sigma_0 = 10^4\,\Omega^{-1}cm^{-1}$, $1/2\pi\tau = 100\,cm^{-1}$, and the c-axis response was taken as $\sigma_{1,c} = 0.5\,\Omega^{-1}cm^{-1}$ and $\varepsilon_{1,c} = 8$ (i.e. $\sigma_c = \sigma_{1,c} - i\omega\varepsilon_0\varepsilon_{1,c}$). Evidently, the solid curve ($\alpha = 0$) represents the Drude response and closely resembles the in-plane conductivity of Fig. 2 (left panels, $T = 50\,K$). Already for small tilt angle the effective conductivity reveals a pronounced peak in the real part of the conductivity, which for $\alpha = 1°$ shows the same shape as the spectra in the right panels of Fig. 2.

Comparative analysis of the in-plane and the mixed response allows to extract the c-axis conductivity of LCCO inverting Eq. (3). Because the spectra for both orientations show only weak deviations at high frequencies, this procedure reveals reliable data below $\nu \sim 30\,cm^{-1}$ only. The c-axis response of LCCO, obtained in this way, is shown in Fig. 4. The dielectric permittivity above T_c is approximately frequency and temperature independent with $\varepsilon_1 \simeq 8$ and $\sigma_1 \simeq 0.5\,\Omega^{-1}cm^{-1}$. An additional contribution to ε_1 due to the superconducting condensate, which is proportional to $-c^2/(\omega\lambda)^2$, starts to grow below T_c. Here λ is the temperature-dependent c-axis penetration depth, which attains the value of $\lambda = 48\,\mu$ for $T \to 0$. Correspondingly, a zero crossing of the dielectric constant is observed in the submillimeter frequency range, which represents a Josephson plasma resonance. This resonance is most clearly seen in the $Im(-1/\varepsilon^*)$ presentation as a sharp maximum close to $\nu \simeq 11.7\,cm^{-1}$.

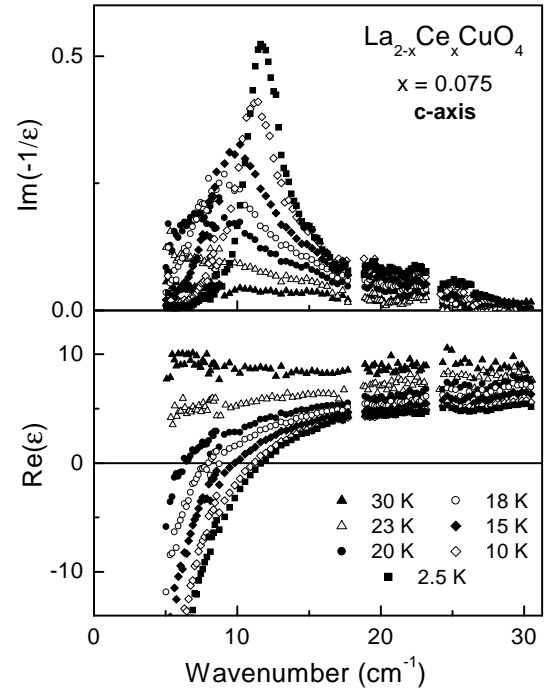In conclusion, we presented the submillimeter-wave

FIG. 4: Dielectric loss function and dielectric permittivity of LCCO along the c-axis. The peak in the loss function corresponds to the Josephson plasma resonance.

and far-infrared conductivity of a $La_{2-x}Ce_xCuO_4$ film measured in a tilted geometry. A broad maximum in the far-infrared conductivity can be observed within this geometry and is attributed to the admixing of the c-axis response to the in-plane conductivity. The same effects can be expected for strongly anisotropic metals, where highly conducting response along one optical axis coexists with almost insulating behavior for another direction. In addition, from the analysis of the mixed and the in-plane contributions the pure c-axis properties of LCCO can be extracted from the spectra, which show a Josephson plasma resonance in the superconducting state.

[1] D. B. Tanner and T. Timusk in *Physical Properties of high Temperature Superconductors III*, edited by D. M. Ginsberg (World Scientific, Singapore, 1992), p. 363.
[2] A. Pimenov *et al.*, Phys. Rev. B **61**, 7039 (2000).
[3] A. Pimenov *et al.*, Phys. Rev. B **62**, 9822 (2000).
[4] D. N. Basov, B. Dabrowski, and T. Timusk, Phys. Rev. Lett. **81**, 2132 (1998).
[5] J. J. McGuire *et al.*, Phys. Rev. B **62**, 8711 (2000).
[6] A. V. Puchkov *et al.*, Phys. Rev. B **51**, 3312 (1995).
[7] E. J. Singley *et al.*, Phys. Rev. B 64, 224503 (2001).
[8] W. A. Atkinson and P. J. Hirschfeld, Phys. Rev. Lett. **88**, 187003 (2002).
[9] C. Bernhard *et al.*, Sol. State. Comm. **121**, 93 (2002).
[10] M. Dumm *et al.*, Phys. Rev. Lett. **88**, 147003 (2002).
[11] M. Naito and M. Hepp, Jpn. J. Appl. Phys. **39**, L485 (2000).
[12] M. Naito and M. Hepp, Physica C **357-360**, 333 (2001).
[13] A. Pimenov, A. Loidl and S. I. Krasnosvobodtsev , Phys. Rev. B **65**, 172502 (2002).
[14] G. V. Kozlov and A. A. Volkov in *Millimeter and Submillimeter Wave Spectroscopy of Solids*, edited by G. Grüner (Springer, Berlin, 1998), p.51.
[15] O. S. Heavens, *Optical properties of thin solid films* (Dover Publ., New York, 1991).
[16] A. Pimenov *et al.*, Appl. Phys. Lett. **77**, 429 (2000).